Published in AJSE, Vol:22, Issue: 3
Received on 8th December 2022
Revised on 17th September 2023
Accepted on 3rd December 2023

AIUB JOURNAL OF SCIENCE AND ENGINEERING
ISSN: 1608 – 3679 (print) 2520 – 4890 (Online)

Calibration and Validation of INA219 as Sensor Power Monitoring System using Linear Regression

Farah Yuki Prasetyawati, Dewanto Harjunowibowo, Ahmad Fauzi, Bayu Utomo, and Dani Harmanto

***Abstract*—This paper introduces an innovative approach utilizing the INA219 sensor and ESP8266 for an efficient power monitoring system, complemented by straightforward calibration and validation techniques. Real-time data is seamlessly stored and displayed in Google Sheets through Blynk apps. The system undergoes calibration using fixed DC lamps and resistors as voltage loads, with digital multimeters, oscilloscopes, and power data loggers employed for comparative analysis. Calibration employs the linear regression technique, and accuracy, precision, and uncertainty analyses are determined through Mean Absolute Percent Error (MAPE), Relative Standard Deviation (RSD), and Gaussian distribution. Notably, the load voltage and shunt voltage sensor coefficients of determination (R^2) stand at 0.999 and 0.997, with corresponding accuracy rates of 99.27% and 93.71%, precision levels of 99.82% and 99.55%, and uncertainties of 0.37 V and 0.89 mV. The research reveals a noteworthy finding: for achieving accurate current measurements when employing an external shunt resistor smaller than the INA219's internal shunt resistor, calculating the current using Ohm's law, proves more accurate than direct measurement.**

***Index Terms*—Arduino, Calibration, INA219, Power Logger, Internet of Things.**

I. Introduction

ELECTRICAL energy is indispensable for all communities, necessitating a reliable energy supply to support sustainable economic growth. The escalating demands, attributed to population growth and economic expansion, have led to a 2.7% increase in electrical energy consumption in numerous countries, particularly in developing nations [1]–[3] including for heating and cooling [4]. Utilizing smart meter may help this situation better in terms of efficiency due to its accuracy.

Energy meters typically possess permanent installation characteristics and are limited to close-range monitoring [5, 6]. Although ZigBee, GSM, and RFID modules have been developed for electricity meters [7], their maintenance costs are substantial [7, 8]. The Internet of Things (IoT) emerges as a promising solution, offering more effective and real-time data transmission and communication capabilities, even across long distances [9, 10]. Wireless Fidelity (Wi-Fi) and mobile phone-based data transmission demonstrate potential reductions in daily and weekly electricity consumption by 15.88% and 6.43%, respectively [12].

ESP8266 has advantages over Bluetooth and ZigBee [13]–[15] since wireless data transmission is of higher quality than with Bluetooth and ZigBee modules. Thus, ESP32 and ESP8266 is increasingly used gaining prominence in optimizing IoT systems [13]–[16]. ESP8266, an affordable Wi-Fi technology, governs sensors in IoT automation, with each sensor connecting to the ESP8266 board through General-Purpose Input/Output (GPIO) pins [17], [18]. Rizkyanto et al. [19] used INA219 sensor for a wireless-based power monitoring system for controlling used electrical loads as a load power controller. However, limitations exist in data storage due to the SD Card's capacity.

Thus, IoT facilitates collaboration between major companies such as Amazon, IBM, and Microsoft, utilizing cloud data management and Google's cloud storage. Google Sheets, provides real-time access and modification of Google Apps Scripts (GAS), demonstrating shorter database connection and data retrieval times compared to MySQL [21]. GAS governs the direction of Hypertext Transfer Protocol (HTTP) data communication, integrating with the Application Programming Interface (API) connected to the HTTP communication protocol in GAS [22]–[24].

Based on a potential analysis, diverse voltage and current measurements have been implemented in an electric power monitoring system [13], [25]. The datasheet [26] reveals that the sensor has the potential to serve as a reliable DC power meter component, with a maximum error rate of 0.5%. The INA219, as described in the datasheet, is capable of measuring voltage drops across a shunt resistor in circuits where the voltage does not exceed 26 V. Additionally, the INA219 can simultaneously measure currents up to 3.2A and integrate with other IoT devices for a low-cost smart home system [27]. Furthermore, Murti et al. [20] developed a measuring instrument using sensor types CR5310-300 and WCS1800, achieving calibration accuracy rates of 99.99% for voltage and 99.98% for current. Notably, the datasheet lacks details on a calibration system. Whereas, calibration is imperative for all electricity-monitoring instruments to prevent measurement deviations, encompassing both DC and AC measuring instruments. Hence, calibration being fundamental to measurement management, ensures the accuracy, reliability, and traceability of measurement tools.

Consequently, this research contributes to develop and

Farah Yuki Prasetyawati
Physics Education Department, Sebelas Maret University, Indonesia.
E-mail: farahyuki.fyp.fyp@gmail.com
Dewanto Harjunowibowo
Physics Education Department, Sebelas Maret University, Indonesia.
E-mail: dewanto_h@staff.uns.ac.id
Ahmad Fauzi
Physics Education Department, Sebelas Maret University, Indonesia.
Bayu Utomo
Electrical, Energy, and Environment Research Group, National Research and Innovation Agency (BRIN), Indonesia.
Dani Harmanto ·
Aeronautical Engineering, De Montfort University, United Kingdom.

propose a simple calibration method for a power monitor. This involves simultaneous real-time measurement of current and voltage in a single component connected to the Blynk and Google Sheets platforms via IoT. The developed system undergoes calibration and validation to assess its feasibility for mass deployment.

II. Materials And Method

A. Research Design

The power monitoring system is designed to operate in real-time utilizing various hardware components as detailed in **Error! Reference source not found.**, **Error! Reference source not found.**, and TABLE III. **Error! Reference source not found.** shows a flowchart algorithm illustrates the interplay between the software and hardware employed in the power monitoring system. The INA219 sensor serves as the primary component in this system, responsible for measuring bus voltage (BV), load voltage (LV), shunt voltage (SV), current (I), and DC power (P). The measurement results are displayed on the Arduino IDE application's serial monitor. Subsequently, the results for each type undergo calibration and validation processes. Following this, the data is transmitted to the Blynk and Google Sheets platforms, establishing connections through the GAS and Arduino programming.

TABLE I
Main Components

No.	Materials	Qty.
1.	Sensor INA219	1
2.	NodeMCU ESP8266 V3	1

TABLE II
Static Load

No.	Materials	Qty.	Measurement
1.	Resistor 4.7KΩ	1	Vrms calibration
2.	Green LED 3V	1	
3.	Shunt resistor 0.01Ω	1	Vdrop calibration
4.	LED 12V 25W	1	
5.	DC lamp 9W 12V	3	Maximum voltage
6.	DC Pump 12V 5A	1	Inductive load

TABLE III
Standardised Reference Instruments

No.	Materials	Qty.
1.	Hantek 365D Bluetooth/USB Data Logger	1
2.	SANWA Digital Multimeter CD800a	1
3.	GWInstek GDS-1120B Oscilloscope	1
4.	DC Power Supply MDB-3010EC	1

B. Hardware Design

The INA219 sensor is linked to the NodeMCU ESP8266, receiving a positive input from the power supply (Vin+) and a negative input from the load (Vin-) as seen in Fig. 2. The input from the power supply (V1) can be adjusted based on the load requirements for accurate measurements. The INA219 generates a voltage drop across the input Vin+ and Vin-, directing it to the internal shunt resistor. Simultaneously, the voltage Vin- connected to GND serves as a parameter determining the magnitude of the bus voltage value. Both Vin+ and Vin- represent analog voltages from the load, requiring conversion to digital using the internal ADC of the INA219 sensor. Additionally, proper connection of all ground pins, is essential to prevent measurement errors.

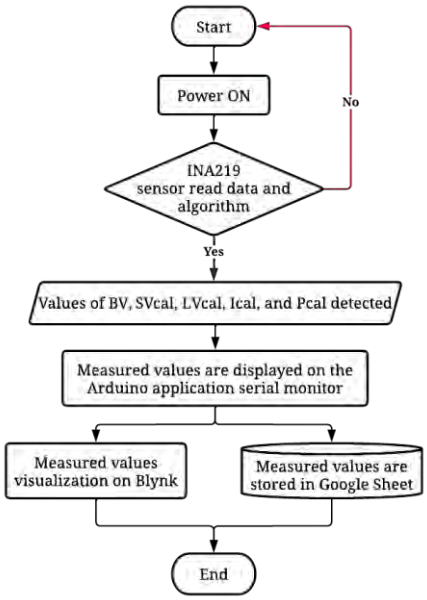

Fig. 1. The algorithm flowchart of power monitoring system

That configuration allows the NodeMCU to receive, process, store, and transmit the measurement data of a load's power consumption via Wi-Fi to various platforms and data storage. The NodeMCU adhering to the 802.11 b/g/n antenna protocol, operating on the ISM 2.4GHz frequency, with an operating current of 80mA, operating voltage range of 2.5-3.6V, a CPU type Tensilica L106 32-bit processor, and PA + 25dBm.

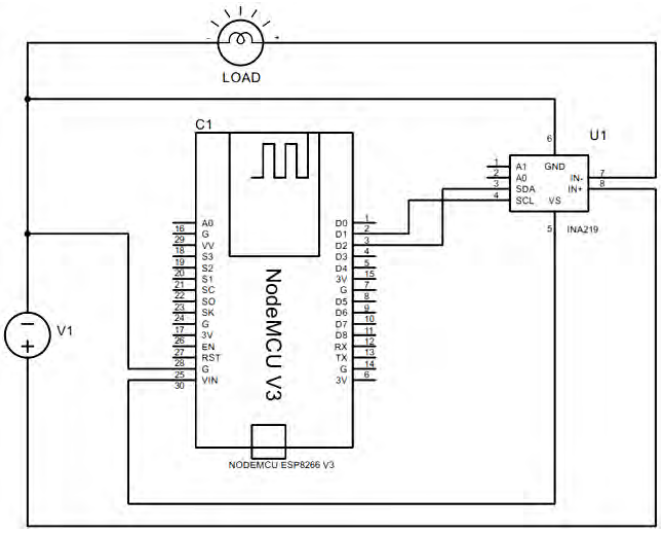

Fig. 2. Schematic circuit of Power Monitoring System

C. Software Design

The NodeMCU, ensures consistent real-time data views across both Blynk and Google Sheets, displaying measurement results (bus voltage, shunt voltage, load voltage, current, and power) along with corresponding delivery times.

1) Blynk IoT platform

Blynk version 1.0.1 facilitates the connection of User Interface (UI) designs for both mobile application and website. This is achieved by modifying data-sending commands from NodeMCU, activated with TemplateID and AuthToken

2) Google sheets

Google Sheets serves as a real-time data storage platform.

Apps Script facilitates NodeMCU interaction with Google Sheets cells, rows, and columns, ensuring accurate input of measured values. Apps Script requires code sequences including SheetID, Sheet Name, developer-localized time, and measurement type. The software developed generates a Deployment ID and URL, which can be input into the Arduino IDE program, enabling real-time integration with Blynk and other hardware.

D. Calibration

These investigations involve the calibration of load voltage RMS (Vrms) and voltage drop (Vdrop) measurements. Fig. 3 illustrates calibration with the Power Monitoring System, Fig. 4 demonstrates calibration with a multimeter, and Fig. 5 depicts calibration with a data logger.

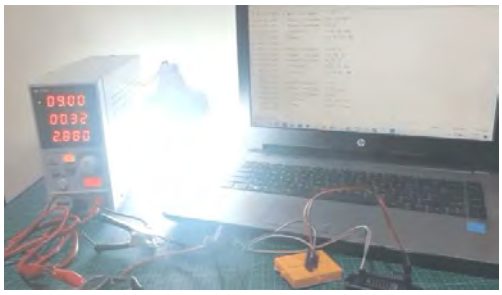

Fig. 3. Calibration with Power Monitoring System

Fig. 4. Calibration with Multimeter and Oscilloscope

Fig. 5. Calibration with Data Logger

Fig. 2 also illustrates the schematic wiring for the Vrms calibration circuit, and Fig. 6 depicts the schematic wiring for the Vdrop calibration circuit. Vrms was calibrated using a 1V to 15V input range with a 4.7KΩ resistor and a 3V LED load. For Vdrop calibration, a 7.7V to 9.1V input range was employed with a 0.01Ω shunt resistor and a 12V LED as the load. The input voltage range for Vdrop calibration was set between 7.7V and 9.1V. Both Vrms calibration and Vdrop calibration utilize specific measuring tools—an oscilloscope for Vrms and a Hantek data logger for Vdrop. Fifteen sets of calibration data are collected for each input voltage.

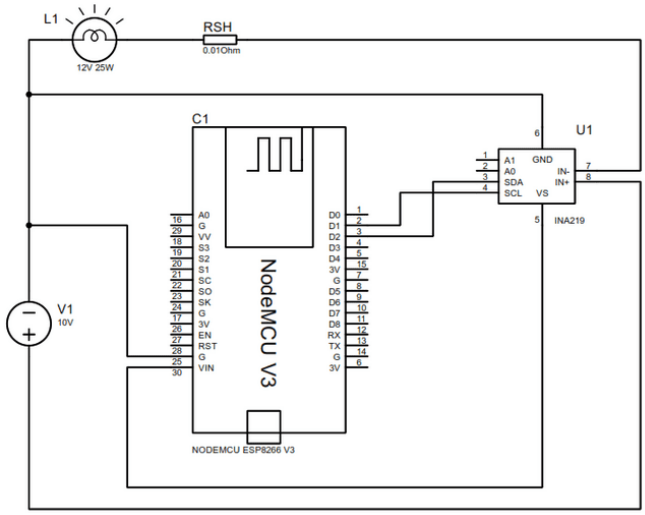

Fig. 6. Schematic wiring of Vdrop calibration.

E. Data Validity

Standardized measuring instruments, such as a data logger, multimeter, and oscilloscope, were utilized to validate the latest values obtained from this calibration. The validation process included the analysis of error, precision, accuracy, and uncertainty.

F. Mean Absolute Percentage Error (MAPE)

MAPE (Mean Absolute Percentage Error) is a method for calculating absolute error, offering an accurate measurement independent of the variable's size or the scale of the predicted demand. This characteristic makes it simple to interpret and consistently applicable across different scales. MAPE generates an error value by comparing the expected value (F) to the observed or actual value (A). The greater the MAPE value, the lower the accuracy of the measuring device in producing a quantitative reading [28].

$$MAPE = \frac{1}{N}\sum_{i=1}^{N}\left|\frac{A_i - F_i}{A_i}\right| \times 100\% \quad (1)$$

$$accuracy = 100\% - MAPE \quad (2)$$

MAPE is expressed as a single-valued error follows $MAPE = \frac{1}{N}\sum_{i=1}^{N}\left|\frac{A_i - F_i}{A_i}\right| \times 100\%$ (**1**) [29]–[32]. Additionally, MAPE is only applicable when the actual value is not zero; it yields an infinite value when the actual value is zero [24]. The accuracy value is determined by the MAPE percentage follows $accuracy = 100\% - MAPE$ (**2**) [26, 27], and TABLE IV classifies MAPE accordingly.

TABLE IV
MAPE CLASSIFICATION [35]

Indicator	Classification
$MAPE \le 10\%$	High
$10\% < MAPE \le 20\%$	Good
$20\% < MAPE \le 50\%$	Reasonable
$MAPE > 50\%$	Inaccurate

G. Precision

A precision analysis was conducted to assess the closeness of data obtained from repeated measurements under consistent conditions [34]. Standard Deviation (SD) and Relative Standard Deviation (RSD) were utilized to evaluate the accuracy of a measuring instrument. SD is commonly employed to identify patterns of distribution and variability. Equation (**3**) represents the SD (σ) with $N-1$ as the number of degrees of freedom, and $\bar{x}$ as the average sensor measurement value formulated as (**4**). Here, x_i represents the value of each sensor measurement, and N is the total number of measurements [36].

$$\sigma = \sqrt{\frac{\sum_{i=1}^{N}\left(x_i - \bar{x}\right)^2}{N-1}} \quad (3)$$

$$\bar{x} = \frac{\sum_{i=1}^{N} x_i}{N} \quad (4)$$

Equation (**5**) is the mathematical equation of RSD, hence, Precision is obtained by using (**6**).

$$RSD = \frac{\sigma}{\bar{x}} \times 100\% \quad (5)$$

$$precision = 100\% - RSD \quad (6)$$

H. Uncertainty

Uncertainty is determined through the Gaussian distribution method by calculating the mean and standard deviation expressed through (**7**) [37], [38]. U_x is uncertainty, σ_N is SD of a certain number of N measurements, and $\overline{X_N}$ is the average of some N measurements.

$$U_x = \pm\left(2\frac{\sigma_N}{X_N}\right) \times 100 \quad (7)$$

III. Result And Discussions

A. Power Monitoring System Design

The Power Monitoring System was constructed utilizing the NodeMCU to optimize IoT-based communication systems. IoT functionality was implemented through the Blynk mobile apps (Fig. 7) and website platform (Fig. 8). Information received by Blynk was influenced by adjustments in firmware configuration, AuthTokens, the implementation of libraries, and sequences of commands in code form. Furthermore, the layout patterns of widgets enable flexible monitoring over extended distances, contingent on the availability of an internet connection.

The C++ programming code on the Arduino IDE was employed for measuring bus voltage, load voltage, shunt voltage, current, and power values from the INA219 sensor. This code structure also serves as a command to send real-time data to Blynk and store it in Google Sheets.

Based on the compiled code structure, the delay in displaying measured data on the Arduino IDE and Blynk serial monitors was set to 10 seconds. Although the display time in Google Sheets varied by several milliseconds, this discrepancy was attributed to the data loading process. The delay between data displays aligns consistently with the output values on the serial monitor. Due to the system's rounding of numbers, there is a slight variation between the display on Blynk and the serial monitor.

The Apps Script program in the Google Sheets extension plays a crucial role in influencing the data transmission procedure from the ESP8266. This program has been modified to accommodate the measurement type displayed on the Google Sheets page. Additionally, the time and date are adjusted based on the time zone where the data is collected or monitored.

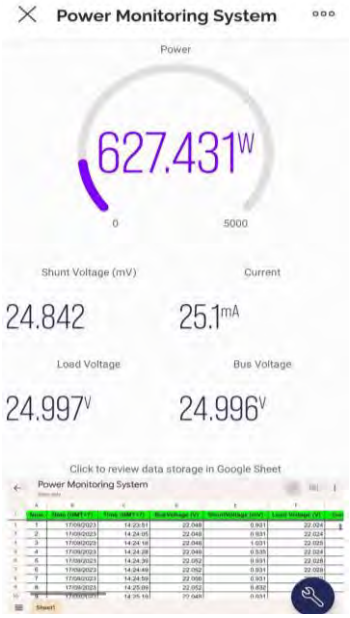

Fig. 7. Power monitoring system in Blynk mobile apps

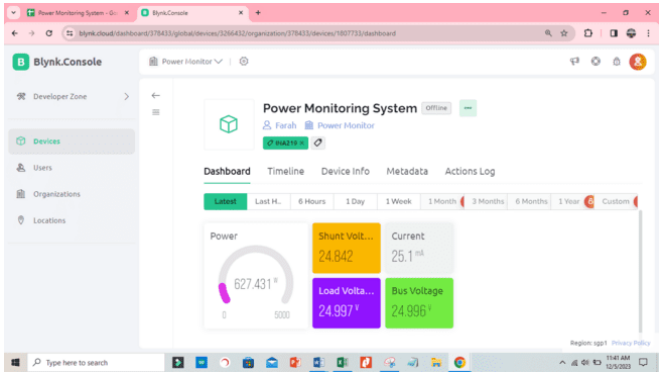

Fig. 8.Power monitoring system in Blynk website

B. Calibration

1) Voltage

Calibration was performed on the load voltage, given its direct relationship with the load. The results of the initial voltage measurement before calibration are presented in

TABLE V. V_M, V_{osc}, V_I, and V_D respectively are voltage measured using multimeter, oscilloscope, INA219, and Hantek data logger.

TABLE V
VOLTAGE MEASUREMENT RESULTS BEFORE CALIBRATION

Input (V)	V_M (V)	V_{osc} (V)	V_I (V)	V_D(V)
1	0.999	0.976	0.985	1.006
2	1.990	1.989	1.983	2.017
3	3.000	2.969	2.979	3.031
4	3.996	3.975	3.995	4.038
5	4.988	4.989	4.871	5.049
6	5.999	6.000	5.968	6.042
7	7.001	7.013	6.980	7.053
8	7.991	8.038	7.983	8.060
9	8.998	9.060	8.985	9.060
10	9.981	10.000	10.010	10.071
11	10.984	11.000	10.999	11.070
12	12.000	11.900	12.000	12.038
13	12.998	13.000	13.003	13.082
14	14.000	14.100	13.990	14.095
15	15.000	15.000	14.979	15.111

Data in
TABLE V were plotted as graphs as shown in Fig. 9 and generates linear equations for the INA219 sensor, multimeter, and data logger which is shown in

$$y_I = 1.0003\,x - 0.0311 \quad (8),$$

$$y_M = 0.9973\,x - 0.0164 \quad (9), \text{ and}$$

$$y_D = 1.0029\,x - 0.031 \quad (10).$$

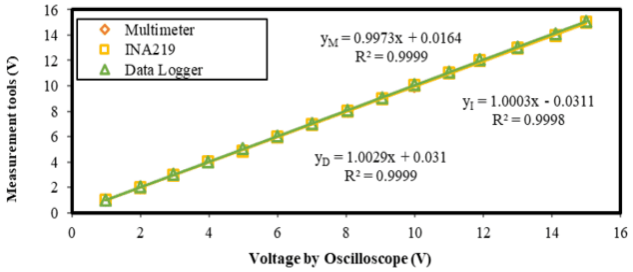

Fig. 9. Before calibrated load voltage graph

$$y_I = 1.0003\,x - 0.0311 \quad (8)$$

$$y_M = 0.9973\,x - 0.0164 \quad (9)$$

$$y_D = 1.0029\,x - 0.031 \quad (10)$$

The three linear equations facilitating calibration through a simple linear calibration technique. In this method, the initial voltage measurement results were substituted to its linear equation as the value of the x variable and replotted as a new graph, as shown in Fig. 10, resulting in voltage calibration determination coefficient of 0.9999 and better intercept. It is evident that both the multimeter and data logger obtained the same coefficient of determination as the INA219 sensor. These coefficients of determination indicate high quality, given their proximity to one [39]. Afterwards, the system can be used for load voltage measurement by utilizing the equation to produce final measurement.

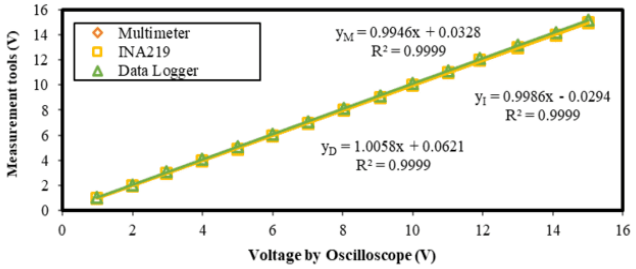

Fig. 10. Calibrated load voltage graph

To assess the built system's voltage measurement capability, deeper tests were conducted using DC lamps as the load. The input voltage was varied from 22V to 32V in one-volt increments. Despite the INA219 sensor's specified maximum limit for measuring Vrms being 26V according to the datasheet, the system demonstrated the ability to measure voltages up to 32V, as depicted in the positive linear graph in Fig. 11.

Furthermore, to assess the impact of calibration, Fig. 12 illustrates the measuring current resulting from voltage calibration. It is evident that the current calculated from the calibrated voltage using Ohm's Law exhibits a consistent trendline for all meters, with a determination coefficient of 0.9998. This indicates that the system has been successfully calibrated and ready for the next field test.

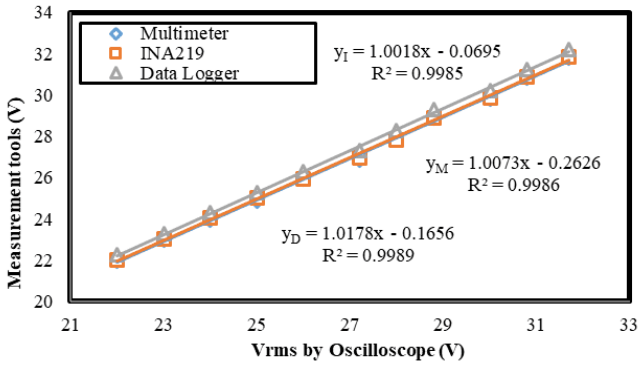

Fig. 11. Vrms measurement.

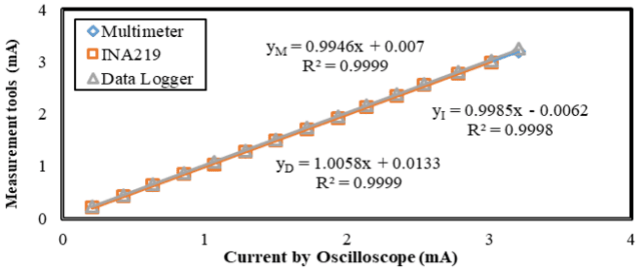

Fig. 12. Current calculation based on calibrated voltage

2) Voltage Drop (Vdrop)

The INA219 sensor also generates a shunt voltage parameter known as voltage drop. Vdrop calibration is employed to derive the current value using Ohm's Law. The voltage drop value is directly proportional to the current value detected by the INA219 sensor in the constructed system. The Vdrop of this system was calibrated using a reference measuring instrument, namely the Hantek 365D Data Logger (V_{dD}). The calibration results (V_{dI}) were then compared with the voltage drop measurements obtained from the Multimeter (V_{dM}), as shown in TABLE VII.

TABLE VI

THE INITIAL VOLTAGE DROP MEASUREMENT BEFORE CALIBRATION

Input (V)	V_{dM} (mV)	V_{dD} (mV)	V_{dI} (mV)
7.7	0.107	0.133	2.019
7.8	0.300	0.273	3.535
7.9	0.447	0.453	5.341
8.0	0.653	0.653	6.365
8.1	0.907	0.900	7.929
8.2	1.120	1.080	11.647
8.3	1.393	1.367	13.828
8.4	1.673	1.673	16.389
8.5	1.940	1.927	18.961
8.6	2.260	2.200	22.886
8.7	2.527	2.487	25.202
8.8	2.893	2.800	28.183
8.9	3.167	3.100	30.663
9.0	3.413	3.373	33.533
9.1	3.693	3.600	36.715

TABLE VI shows the initial voltage drop measurement before calibration. The data were plotted into Fig. 13 produces an INA219's linear equation of $y_I = 0.9213\,x - 0.3362$. It can be seen from Fig. 13 that before calibration, the multimeter and data logger measurement exhibited a significant divergence in trend. Thus, for every built system, calibration is supercritical to be conducted.

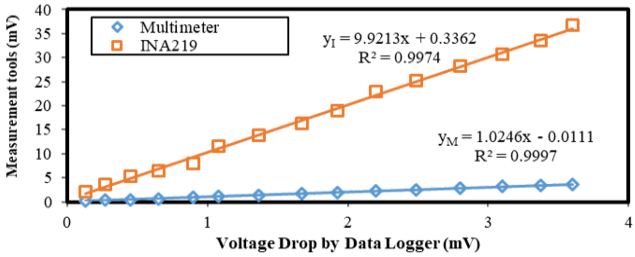

Fig. 13. Before calibration voltage drop graph.

Likewise explained voltage calibration, substituting the old I_{dI} value into the x in the y_I linear regression obtained, as depicted in Fig. 14, aligns the constructed system well with both the multimeter and the data logger. The R^2 for INA219, multimeter, and Data Logger is close to one, signifying that the built system is now more valid for Vdrop measurements.

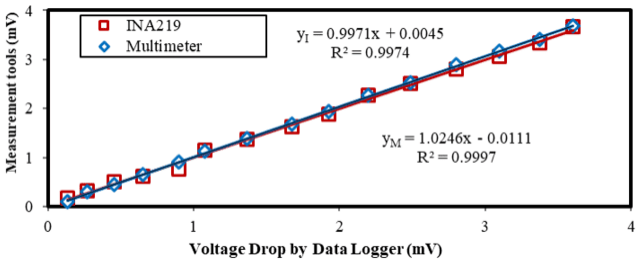

Fig. 14. Calibrated voltage drop graph

However, when it is used to measure current after the calibration, using a 0.01Ω resistance, results in an average error of 0.1mV in the measured voltage drop. The failure was suspected to be due to the INA's shunt (0.1Ω) being larger than the used shunt resistor, causing measurement errors. To address this issue, the current to be measured can be calculated using Ohm's law from the measured Vdrop, as detailed in TABLE VII. I_{Ical}, I_D, and I_M represent the current measured with the calibrated INA219, data logger, and multimeter, respectively. As the results, the voltage drop calibration produced identical measurement results to those obtained from other meters as shown in Fig. 15.

TABLE VII

CALCULATION CURRENT FROM VOLTAGE DROP

Input (V)	$I_{I\,cal}$ (mA)	I_D (mA)	I_M (mA)
7.7	17.364	13.333	10.667
7.8	32.600	27.333	30.000
7.9	50.744	45.333	44.667
8.0	61.042	65.333	65.333
8.1	76.753	90.000	90.667
8.2	114.119	108.000	112.000
8.3	136.041	136.667	139.333
8.4	161.783	167.333	167.333
8.5	187.625	192.667	194.000
8.6	227.074	220.000	226.000
8.7	250.350	248.667	252.667
8.8	280.313	280.000	289.333
8.9	305.237	310.000	316.667
9.0	334.073	337.333	341.333
9.1	366.052	360.000	369.333

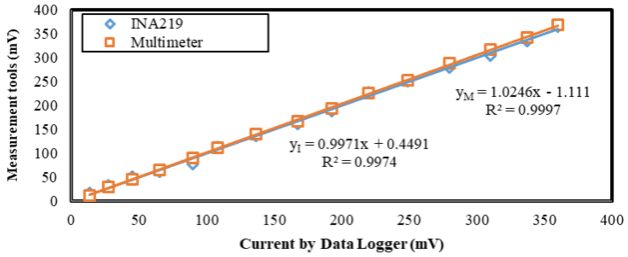

Fig. 15. Current resulted from calibrated voltage drop

C. *Validation*

This stage focused on evaluating the accuracy, precision, and uncertainty of the built system's measurements in comparison to other meters.

1) *Accuracy*

The MAPE method was employed to assess the proximity of INA219 measurement results after calibration with the multimeter, INA219 sensor, data logger, and oscilloscope. Error and accuracy measurements were utilized to calculate the results, as illustrated in TABLE VIII. The calculations reveal that the multimeter exhibits the highest accuracy for measuring both voltage and voltage drop. Furthermore, the INA219 is more accurate than the Data Logger in measuring load voltage.

TABLE VIII
VOLTAGE MEASUREMENT MAPE AND ACCURACY

Type	Voltage		Voltage Drop	
Benchmark	Oscilloscope		Data Logger	
Analysis	MAPE (%)	Accuracy (%)	MAPE (%)	Accuracy (%)
Multimeter	0.68	99.32	3.70	96.29
INA219	0.73	99.27	6.29	93.71
Data Logger	1.90	98.09	-	-

2) *Precision*

From TABLE IX, the highest precision in voltage measurement is observed with the Hantek data logger, achieving 99.93%. Conversely, the INA219 system exhibits the lowest precision for voltage measurement. On the other hand, when it comes to Vdrop, the INA219 proves to be the most precise instrument. Notably, the oscilloscope couldn't detect the Vdrop due to the small size of the used shunt resistor (0.01Ω).

TABLE IX
VOLTAGE AND VOLTAGE DROP PRECISION

Measurement Type		Voltage	Voltage Drop
Benchmark		Oscilloscope (%)	Data Logger (%)
Precision	Oscilloscope	-	-
	Multimeter	99.89	94.23

	INA219	99.82	99.55
	Data Logger	99.93	-

3) Uncertainty

In terms of uncertainty measurement, TABLE X demonstrates that the INA219 sensor has the lowest voltage uncertainty compared to others. However, for Vdrop measurement, the built system achieved the smallest.

TABLE X
VOLTAGE AND VOLTAGE DROP MEASUREMENTS UNCERTAINTY

Measurement Type		Voltage (V)	Voltage Drop (mV)
Benchmark		Oscilloscope	Data Logger
Uncertainty (±)	Oscilloscope	0.30	39.22
	Multimeter	0.22	11.55
	INA219	0.37	0.89
	Data Logger	0.15	12.17

D. Load Testing

Calibration and validation tests were carried out on the Power Monitoring System using resistive loads, confirming the sensor's capability to measure such loads. Furthermore, inductive load testing was conducted using a pump as the load. As the result illustrated in TABLE XI, Vrms maintained an almost constant value under test circuit conditions with a consistent input voltage and varying input current. The graphic representation of the results in Fig. 16 indicates that the INA219 sensor remains unaffected by loads type.

TABLE XI
VRMS MEASUREMENT WITH INDUCTIVE LOAD

Input (A)	$V_{I\,cal}$ (V)	V_D (V)	I_M (V)
0.50	11.967	12.136	11.964
1.00	11.966	12.136	11.964
1.50	11.966	12.136	11.964
2.00	11.965	12.136	11.964
2.50	11.966	12.136	11.964
3.00	11.965	12.136	11.964

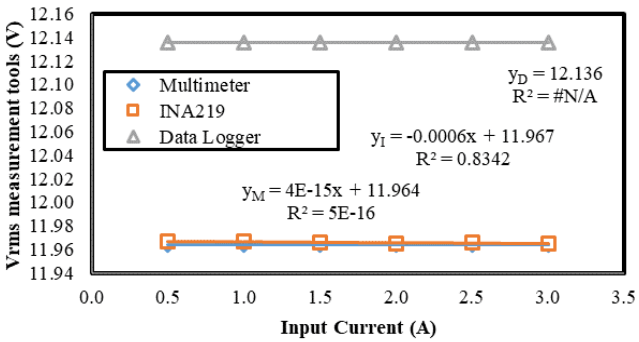

Fig. 16. Inductive load testing

IV. CONCLUSION

This research aims to develop a power monitoring and logging system, showcasing a straightforward calibration and validation technique to ensure accurate measurement results. The built system utilizes the INA219 sensor for detecting DC power, with data collected and visualized in real-time using Google Sheets and Blynk. Calibrations were achieved through a simple linear regression technique on load and shunt voltage, resulting in determination coefficients (R^2) of 0.999 for load voltage and 0.997 for shunt voltage drop, indicating successful calibration. Accuracy tests yielded 99.27% for load voltage and 93.71% for shunt voltage drop. In terms of precision, the sensor demonstrated high precision with 99.82% for measuring voltage and 99.55% for measuring voltage drop, accompanied by uncertainties of 0.37 V and 0.89 mV, respectively. Therefore, this power monitoring system is deemed feasible as a measuring tool due to its high precision and accuracy. For future work, the system could be enhanced with a relay for use in appliances as a power management system. Additionally, this built system can find applications in laboratory work.

ACKNOWLEDGEMENT

The authors thank you Universitas Sebelas Maret and Ministry of Research, Technology and Higher Education Indonesia for Applied Research grant no 469.1/UN27.22/PT.01.03/2022 for the funding supports, and ESMART Research Group for the lab supports.

REFERENCES

[1] T. Ahmad and D. Zhang, 'A critical review of comparative global historical energy consumption and future demand: The story told so far', *Energy Reports*, vol. 6, pp. 1973–1991, Nov. 2020, doi: 10.1016/J.EGYR.2020.07.020.

[2] R. Nepal and N. Paija, 'Energy security, electricity, population and economic growth: The case of a developing South Asian resource-rich economy', *Energy Policy*, vol. 132, no. May, pp. 771–781, 2019, doi: 10.1016/j.enpol.2019.05.054.

[3] G. Karhan, 'Does renewable energy increase growth? Evidence from EU-19 countries', *Int. J. Energy Econ. Policy*, vol. 9, no. 2, pp. 341–346, 2019, doi: 10.32479/ijeep.7589.

[4] D. Harjunowibowo, S. A. Omer, and S. B. Riffat, 'Experimental investigation of a ground-source heat pump system for greenhouse heating-cooling', *Int. J. Low-Carbon Technol.*, vol. 16, no. 4, pp. 1529–1541, 2021, doi: 10.1093/ijlct/ctab052.

[5] M. Y. Al-Shorman, M. M. Al-Kofahi, and O. M. Al-Kofahi, 'A practical microwatt-meter for electrical energy measurement in programmable devices', *Meas. Control (United Kingdom)*, vol. 51, no. 9–10, pp. 383–395, 2018, doi: 10.1177/0020294018794350.

[6] D. Brunelli, C. Villani, D. Balsamo, and L. Benini, 'Non-invasive voltage measurement in a three-phase autonomous meter', *Microsyst. Technol.*, vol. 22, no. 7, pp. 1915–1926, 2016, doi: 10.1007/s00542-016-2890-7.

[7] S. Ansari, A. Ayob, M. S. Hossain Lipu, M. H. Md Saad, and A. Hussain, 'A review of monitoring technologies for solar pv systems using data processing modules and transmission protocols: Progress, challenges and prospects', *Sustain.*, vol. 13, no. 15, 2021, doi: 10.3390/su13158120.

[8] S. Ding, J. Liu, and M. Yue, 'The Use of ZigBee Wireless Communication Technology in Industrial Automation Control', *Wirel. Commun. Mob. Comput.*, vol. 2021, 2021, doi: 10.1155/2021/8317862.

[9] W. Boonsong and W. Ismail, 'Wireless monitoring of household electrical power meter using embedded RFID with wireless sensor network platform', *Int. J. Distrib. Sens. Networks*, vol. 2014, 2014, doi: 10.1155/2014/876914.

[10] M. Bevilacqua, F. E. Ciarapica, C. Diamantini, and D. Potena, 'Big data analytics methodologies applied at energy management in industrial sector: A case study', *Int. J. RF Technol. Res. Appl.*, vol. 8, no. 3, pp. 105–122, 2017, doi: 10.3233/RFT-171671.

[11] K. Luechaphonthara and A. Vijayalakshmi, 'IOT based application for monitoring electricity power consumption in home appliances', *Int. J. Electr. Comput. Eng.*, vol. 9, no. 6, pp. 4988–4992, 2019, doi: 10.11591/ijece.v9i6.pp4988-4992.

[12] L. Martirano *et al.*, 'Assessment for a Distributed Monitoring System for Industrial and Commercial Applications', *IEEE Trans. Ind. Appl.*, vol. 55, no. 6, pp. 7320–7327, 2019, doi: 10.1109/TIA.2019.2939507.

[13] M. K. Hasan, M. M. Ahmed, B. Pandey, H. Gohel, S. Islam, and I. F. Khalid, 'Internet of Things-Based Smart Electricity Monitoring and Control System Using Usage Data', *Wirel. Commun. Mob. Comput.*, vol. 2021, 2021, doi: 10.1155/2021/6544649.

[14] J. Cai and O. C. Ugweje, 'A comparative study of wireless ATM MAC protocols', *2002 Int. Conf. Commun. Circuits Syst. West Sino Expo. ICCCAS 2002 - Proc.*, pp. 516–520, 2002, doi: 10.1109/ICCCAS.2002.1180671.

[15] O. O. Kazeem, L. O. Kehinde, O. O. Akintade, and L. O. Kehinde,

'Comparative Study of Communication Interfaces for Sensors and Actuators in the Cloud of Internet of Things', *Int. J. Internet Things*, vol. 2017, no. 1, pp. 9–13, 2017, doi: 10.5923/j.ijit.20170601.02.

[16] J. M. Ramadhan, R. Mardiati, and I. N. Haq, 'IoT Monitoring System for Solar Power Plant Based on MQTT Publisher / Subscriber Protocol', in *2021 7th International Conference on Wireless and Telematics (ICWT)*, Bandung, Indonesia, 2021, pp. 1–6. doi: 10.1109/ICWT52862.2021.9678503.

[17] A. Yudidharma, N. Nathaniel, T. N. Gimli, S. Achmad, and A. Kurniawan, 'A systematic literature review: Messaging protocols and electronic platforms used in the internet of things for the purpose of building smart homes', *Procedia Comput. Sci.*, vol. 216, no. 2022, pp. 194–203, 2023, doi: 10.1016/j.procs.2022.12.127.

[18] M. E. S. M. Essa *et al.*, 'Reliable Integration of Neural Network and Internet of Things for Forecasting, Controlling, and Monitoring of Experimental Building Management System', *Sustain.*, vol. 15, no. 3, 2023, doi: 10.3390/su15032168.

[19] M. Rizkyanto, A. Hariyadi, and N. Suharto, 'Design and Development of Wireless-Based Electric Load Control Monitoring System on Autobuses Vehicles', *J. Jartel J. Jar. Telekomun.*, vol. 12, no. 4, pp. 270–275, 2022, doi: 10.33795/jartel.v12i4.508.

[20] S. Murti, P. Megantoro, G. De Brito Silva, and A. Maseleno, 'Design and analysis of DC electrical voltage-current data logger device implemented on wind turbine control system', *J. Robot. Control*, vol. 1, no. 3, pp. 75–80, 2020, doi: 10.18196/jrc.1317.

[21] L. J. Ekanayake, D. Ihalage, and S. P. Abyesundara, 'Performance Evaluation of Google Spreadsheet over RDBMS through Cloud Scripting Algorithms', *2021 Int. Conf. Comput. Commun. Informatics, ICCCI 2021*, pp. 1–7, 2021, doi: 10.1109/ICCCI50826.2021.9402432.

[22] T. DeBell, L. Goertzen, L. Larson, W. Selbie, J. Selker, and C. Udell, 'OPEnS hub: Real-time data logging, connecting field sensors to google sheets', *Front. Earth Sci.*, vol. 7, no. May, pp. 1–6, 2019, doi: 10.3389/feart.2019.00137.

[23] R. Z. Fitriani, C. B. D. Kuncoro, and Y. Der Kuan, 'Internet-based remote setting and data acquisition for fuel cell', *Sensors Mater.*, vol. 33, no. 11, pp. 3903–3915, 2021, doi: 10.18494/SAM.2021.3630.

[24] S. Abdullah, A. Daud, N. S. Mohamad Hadis, S. A. Hamid, S. Y. Fadhlullah, and N. S. Damanhuri, 'Internet of Things (IoT) Based Smart Shop (S-SHOP) System with RFID Technique', *J. Phys. Conf. Ser.*, vol. 1535, no. 1, p. 012011, May 2020, doi: 10.1088/1742-6596/1535/1/012011.

[25] Y. Cheddadi, H. Cheddadi, F. Cheddadi, F. Errahimi, and N. Es-sbai, 'Design and implementation of an intelligent low-cost IoT solution for energy monitoring of photovoltaic stations', *SN Appl. Sci.*, vol. 2, no. 7, pp. 1–11, 2020, doi: 10.1007/s42452-020-2997-4.

[26] Texas Instruments, 'Bidirectional Current/Power Monitor INA219 Datasheet', no. December. Texas Instruments, p. 39, 2015. [Online]. Available: http://www.ti.com/lit/ds/symlink/ina219.pdf

[27] A. Howedi and A. Jwaid, 'Design and implementation prototype of a smart house system at low cost and multi-functional', *FTC 2016 - Proc. Futur. Technol. Conf.*, no. December, pp. 876–884, 2017, doi: 10.1109/FTC.2016.7821706.

[28] P. Panja, W. Jia, and B. McPherson, 'Prediction of well performance in SACROC field using stacked Long Short-Term Memory (LSTM) network', *Expert Syst. Appl.*, vol. 205, p. 117670, Nov. 2022, doi: 10.1016/J.ESWA.2022.117670.

[29] X. Chen, Y. Wang, and J. Tuo, 'Short-term power load forecasting of GWO-KELM based on Kalman filter', *IFAC-PapersOnLine*, vol. 53, no. 2, pp. 12086–12090, Jan. 2020, doi: 10.1016/J.IFACOL.2020.12.760.

[30] A. Ghosh, P. Satvaya, P. K. Kundu, and G. Sarkar, 'Calibration of RGB sensor for estimation of real-time correlated color temperature using machine learning regression techniques', *Optik (Stuttg).*, vol. 258, p. 168954, May 2022, doi: 10.1016/J.IJLEO.2022.168954.

[31] S. Kim and H. Kim, 'A new metric of absolute percentage error for intermittent demand forecasts', *Int. J. Forecast.*, vol. 32, no. 3, pp. 669–679, Jul. 2016, doi: 10.1016/J.IJFORECAST.2015.12.003.

[32] U. Khair, H. Fahmi, S. Al Hakim, and R. Rahim, 'Forecasting Error Calculation with Mean Absolute Deviation and Mean Absolute Percentage Error', *J. Phys. Conf. Ser.*, vol. 930, no. 1, p. 012002, Dec. 2017, doi: 10.1088/1742-6596/930/1/012002.

[33] D. Koutsandreas, E. Spiliotis, F. Petropoulos, and V. Assimakopoulos, 'On the selection of forecasting accuracy measures', *J. Oper. Res. Soc.*, vol. 73, no. 5, pp. 937–954, 2022, doi: 10.1080/01605682.2021.1892464.

[34] J. E. M. Perea Martins, 'Introducing the concepts of measurement accuracy and precision in the classroom', *Phys. Educ.*, vol. 54, no. 5, p. 055029, Sep. 2019, doi: 10.1088/1361-6552/ab3143.

[35] X. Li, A. Ren, and Q. Li, 'Exploring Patterns of Transportation-Related CO2 Emissions Using Machine Learning Methods', *Sustain.*, vol. 14, no. 8, Apr. 2022, doi: 10.3390/SU14084588.

[36] Y. Gao, M. G. Ierapetritou, and F. J. Muzzio, 'Determination of the confidence interval of the relative standard deviation using convolution', *J. Pharm. Innov.*, vol. 8, no. 2, pp. 72–82, Jun. 2013, doi: 10.1007/S12247-012-9144-8/TABLES/3.

[37] D. Harjunowibowo, R. A. B. Prasetyo, F. Ahmadi, T. Rahman, R. N. Wirabuana, and R. Zeinelabdein, 'Improving thermal performance of dwelling single glass windows using secondary glazing in the UK', *Int. J. Adv. Sci. Eng. Inf. Technol.*, vol. 9, no. 4, 2019, doi: 10.18517/ijaseit.9.4.9461.

[38] S. Mukherjee, S. Chakrabarty, P. C. Mishra, and P. Chaudhuri, 'Transient heat transfer characteristics and process intensification with Al2O3-water and TiO2-water nanofluids: An experimental investigation', *Chem. Eng. Process. - Process Intensif.*, vol. 150, Apr. 2020, doi: 10.1016/j.cep.2020.107887.

[39] D. Chicco, M. J. Warrens, and G. Jurman, 'The coefficient of determination R-squared is more informative than SMAPE, MAE, MAPE, MSE and RMSE in regression analysis evaluation', *PeerJ Comput. Sci.*, vol. 7, pp. 1–24, 2021, doi: 10.7717/PEERJ-CS.623/SUPP-1.

[1] T. Ahmad and D. Zhang, 'A critical review of comparative global historical energy consumption and future demand: The story told so far', *Energy Reports*, vol. 6, pp. 1973–1991, Nov. 2020, doi: 10.1016/J.EGYR.2020.07.020.

[2] R. Nepal and N. Paija, 'Energy security, electricity, population and economic growth: The case of a developing South Asian resource-rich economy', *Energy Policy*, vol. 132, no. May, pp. 771–781, 2019, doi: 10.1016/j.enpol.2019.05.054.

[3] G. Karhan, 'Does renewable energy increase growth? Evidence from EU-19 countries', *Int. J. Energy Econ. Policy*, vol. 9, no. 2, pp. 341–346, 2019, doi: 10.32479/ijeep.7589.

[4] D. Harjunowibowo, S. A. Omer, and S. B. Riffat, 'Experimental investigation of a ground-source heat pump system for greenhouse heating-cooling', *Int. J. Low-Carbon Technol.*, vol. 16, no. 4, pp. 1529–1541, 2021, doi: 10.1093/ijlct/ctab052.

[5] M. Y. Al-Shorman, M. M. Al-Kofahi, and O. M. Al-Kofahi, 'A practical microwatt-meter for electrical energy measurement in programmable devices', *Meas. Control (United Kingdom)*, vol. 51, no. 9–10, pp. 383–395, 2018, doi: 10.1177/0020294018794350.

[6] D. Brunelli, C. Villani, D. Balsamo, and L. Benini, 'Non-invasive voltage measurement in a three-phase autonomous meter', *Microsyst. Technol.*, vol. 22, no. 7, pp. 1915–1926, 2016, doi: 10.1007/s00542-016-2890-7.

[7] S. Ansari, A. Ayob, M. S. Hossain Lipu, M. H. Md Saad, and A. Hussain, 'A review of monitoring technologies for solar pv systems using data processing modules and transmission protocols: Progress, challenges and prospects', *Sustain.*, vol. 13, no. 15, 2021, doi: 10.3390/su13158120.

[8] S. Ding, J. Liu, and M. Yue, 'The Use of ZigBee Wireless Communication Technology in Industrial Automation Control', *Wirel. Commun. Mob. Comput.*, vol. 2021, 2021, doi: 10.1155/2021/8317862.

[9] W. Boonsong and W. Ismail, 'Wireless monitoring of household electrical power meter using embedded RFID with wireless sensor network platform', *Int. J. Distrib. Sens. Networks*, vol. 2014, 2014, doi: 10.1155/2014/876914.

[10] M. Bevilacqua, F. E. Ciarapica, C. Diamantini, and D. Potena, 'Big data analytics methodologies applied at energy management in industrial sector: A case study', *Int. J. RF Technol. Res. Appl.*, vol. 8, no. 3, pp. 105–122, 2017, doi: 10.3233/RFT-171671.

[11] K. Luechaphonthara and A. Vijayalakshmi, 'IOT based application for monitoring electricity power consumption in home appliances', *Int. J. Electr. Comput. Eng.*, vol. 9, no. 6, pp. 4988–4992, 2019, doi: 10.11591/ijece.v9i6.pp4988-4992.

[12] L. Martirano *et al.*, 'Assessment for a Distributed Monitoring System for Industrial and Commercial Applications', *IEEE Trans. Ind. Appl.*, vol. 55, no. 6, pp. 7320–7327, 2019, doi: 10.1109/TIA.2019.2939507.

[13] M. K. Hasan, M. M. Ahmed, B. Pandey, H. Gohel, S. Islam, and I. F. Khalid, 'Internet of Things-Based Smart Electricity Monitoring and Control System Using Usage Data', *Wirel. Commun. Mob. Comput.*, vol. 2021, 2021, doi: 10.1155/2021/6544649.

[14] J. Cai and O. C. Ugweje, 'A comparative study of wireless ATM MAC protocols', *2002 Int. Conf. Commun. Circuits Syst. West*

Sino Expo. ICCCAS 2002 - Proc., pp. 516–520, 2002, doi: 10.1109/ICCCAS.2002.1180671.
[15] O. O. Kazeem, L. O. Kehinde, O. O. Akintade, and L. O. Kehinde, 'Comparative Study of Communication Interfaces for Sensors and Actuators in the Cloud of Internet of Things', *Int. J. Internet Things*, vol. 2017, no. 1, pp. 9–13, 2017, doi: 10.5923/j.ijit.20170601.02.
[16] J. M. Ramadhan, R. Mardiati, and I. N. Haq, 'IoT Monitoring System for Solar Power Plant Based on MQTT Publisher / Subscriber Protocol', in *2021 7th International Conference on Wireless and Telematics (ICWT)*, Bandung, Indonesia, 2021, pp. 1–6. doi: 10.1109/ICWT52862.2021.9678503.
[17] A. Yudidharma, N. Nathaniel, T. N. Gimli, S. Achmad, and A. Kurniawan, 'A systematic literature review: Messaging protocols and electronic platforms used in the internet of things for the purpose of building smart homes', *Procedia Comput. Sci.*, vol. 216, no. 2022, pp. 194–203, 2023, doi: 10.1016/j.procs.2022.12.127.
[18] M. E. S. M. Essa *et al.*, 'Reliable Integration of Neural Network and Internet of Things for Forecasting, Controlling, and Monitoring of Experimental Building Management System', *Sustain.*, vol. 15, no. 3, 2023, doi: 10.3390/su15032168.
[19] M. Rizkyanto, A. Hariyadi, and N. Suharto, 'Design and Development of Wireless-Based Electric Load Control Monitoring System on Autobuses Vehicles', *J. Jartel J. Jar. Telekomun.*, vol. 12, no. 4, pp. 270–275, 2022, doi: 10.33795/jartel.v12i4.508.
[20] S. Murti, P. Megantoro, G. De Brito Silva, and A. Maseleno, 'Design and analysis of DC electrical voltage-current data logger device implemented on wind turbine control system', *J. Robot. Control*, vol. 1, no. 3, pp. 75–80, 2020, doi: 10.18196/jrc.1317.
[21] L. J. Ekanayake, D. Ihalage, and S. P. Abyesundara, 'Performance Evaluation of Google Spreadsheet over RDBMS through Cloud Scripting Algorithms', *2021 Int. Conf. Comput. Commun. Informatics, ICCCI 2021*, pp. 1–7, 2021, doi: 10.1109/ICCCI50826.2021.9402432.
[22] T. DeBell, L. Goertzen, L. Larson, W. Selbie, J. Selker, and C. Udell, 'OPEnS hub: Real-time data logging, connecting field sensors to google sheets', *Front. Earth Sci.*, vol. 7, no. May, pp. 1–6, 2019, doi: 10.3389/feart.2019.00137.
[23] R. Z. Fitriani, C. B. D. Kuncoro, and Y. Der Kuan, 'Internet-based remote setting and data acquisition for fuel cell', *Sensors Mater.*, vol. 33, no. 11, pp. 3903–3915, 2021, doi: 10.18494/SAM.2021.3630.
[24] S. Abdullah, A. Daud, N. S. Mohamad Hadis, S. A. Hamid, S. Y. Fadhlullah, and N. S. Damanhuri, 'Internet of Things (IoT) Based Smart Shop (S-SHOP) System with RFID Technique', *J. Phys. Conf. Ser.*, vol. 1535, no. 1, p. 012011, May 2020, doi: 10.1088/1742-6596/1535/1/012011.
[25] Y. Cheddadi, H. Cheddadi, F. Cheddadi, F. Errahimi, and N. Es-sbai, 'Design and implementation of an intelligent low-cost IoT solution for energy monitoring of photovoltaic stations', *SN Appl. Sci.*, vol. 2, no. 7, pp. 1–11, 2020, doi: 10.1007/s42452-020-2997-4.
[26] Texas Instruments, 'Bidirectional Current/Power Monitor INA219 Datasheet', no. December. Texas Instruments, p. 39, 2015. [Online]. Available: http://www.ti.com/lit/ds/symlink/ina219.pdf
[27] A. Howedi and A. Jwaid, 'Design and implementation prototype of a smart house system at low cost and multi-functional', *FTC 2016 - Proc. Futur. Technol. Conf.*, no. December, pp. 876–884, 2017, doi: 10.1109/FTC.2016.7821706.
[28] P. Panja, W. Jia, and B. McPherson, 'Prediction of well performance in SACROC field using stacked Long Short-Term Memory (LSTM) network', *Expert Syst. Appl.*, vol. 205, p. 117670, Nov. 2022, doi: 10.1016/J.ESWA.2022.117670.
[29] X. Chen, Y. Wang, and J. Tuo, 'Short-term power load forecasting of GWO-KELM based on Kalman filter', *IFAC-PapersOnLine*, vol. 53, no. 2, pp. 12086–12090, Jan. 2020, doi: 10.1016/J.IFACOL.2020.12.760.
[30] A. Ghosh, P. Satvaya, P. K. Kundu, and G. Sarkar, 'Calibration of RGB sensor for estimation of real-time correlated color temperature using machine learning regression techniques', *Optik (Stuttg).*, vol. 258, p. 168954, May 2022, doi: 10.1016/J.IJLEO.2022.168954.
[31] S. Kim and H. Kim, 'A new metric of absolute percentage error for intermittent demand forecasts', *Int. J. Forecast.*, vol. 32, no. 3, pp. 669–679, Jul. 2016, doi: 10.1016/J.IJFORECAST.2015.12.003.
[32] U. Khair, H. Fahmi, S. Al Hakim, and R. Rahim, 'Forecasting Error Calculation with Mean Absolute Deviation and Mean Absolute Percentage Error', *J. Phys. Conf. Ser.*, vol. 930, no. 1, p. 012002, Dec. 2017, doi: 10.1088/1742-6596/930/1/012002.
[33] D. Koutsandreas, E. Spiliotis, F. Petropoulos, and V. Assimakopoulos, 'On the selection of forecasting accuracy measures', *J. Oper. Res. Soc.*, vol. 73, no. 5, pp. 937–954, 2022, doi: 10.1080/01605682.2021.1892464.
[34] J. E. M. Perea Martins, 'Introducing the concepts of measurement accuracy and precision in the classroom', *Phys. Educ.*, vol. 54, no. 5, p. 055029, Sep. 2019, doi: 10.1088/1361-6552/ab3143.
[35] X. Li, A. Ren, and Q. Li, 'Exploring Patterns of Transportation-Related CO2 Emissions Using Machine Learning Methods', *Sustain.*, vol. 14, no. 8, Apr. 2022, doi: 10.3390/SU14084588.
[36] Y. Gao, M. G. Ierapetritou, and F. J. Muzzio, 'Determination of the confidence interval of the relative standard deviation using convolution', *J. Pharm. Innov.*, vol. 8, no. 2, pp. 72–82, Jun. 2013, doi: 10.1007/S12247-012-9144-8/TABLES/3.
[37] D. Harjunowibowo, R. A. B. Prasetyo, F. Ahmadi, T. Rahman, R. N. Wirabuana, and R. Zeinelabdein, 'Improving thermal performance of dwelling single glass windows using secondary glazing in the UK', *Int. J. Adv. Sci. Eng. Inf. Technol.*, vol. 9, no. 4, 2019, doi: 10.18517/ijaseit.9.4.9461.
[38] S. Mukherjee, S. Chakrabarty, P. C. Mishra, and P. Chaudhuri, 'Transient heat transfer characteristics and process intensification with Al2O3-water and TiO2-water nanofluids: An experimental investigation', *Chem. Eng. Process. - Process Intensif.*, vol. 150, Apr. 2020, doi: 10.1016/j.cep.2020.107887.
[39] D. Chicco, M. J. Warrens, and G. Jurman, 'The coefficient of determination R-squared is more informative than SMAPE, MAE, MAPE, MSE and RMSE in regression analysis evaluation', *PeerJ Comput. Sci.*, vol. 7, pp. 1–24, 2021, doi: 10.7717/PEERJ-CS.623/SUPP-1.

Farah Yuki Prasetyawati is a Physics Education student at Sebelas Maret University, Indonesia. She has interests in renewable energy, electronics, and education. Her interest has resulted in academic and non-academic achievements both at national and international levels, published books, scientific articles, and intellectual property rights. Besides being a student, she is also active as a smart city consultant in Surakarta City, Indonesia.

Dewanto Harjunowibowo, completed both his undergraduate and graduate degrees in the Physics Department of the Universitas Gadjah Mada (GMU), Indonesia. The Sustainable Energy Technologies program at the University of Nottingham in the United Kingdom is where he received his PhD in Architecture and Built Environment Department. At Universitas Sebelas Maret (UNS), he has been a physics and application instructor for more than 18 years. He also a reviewer and had numerous articles and books published in prominent national and international journals. His expertise includes heat transfer, sustainable energy technology, Internet of Things, and nearly zero energy building. This article is part of a grant he secured in 2022.

Ahmad Fauzi was born in Semarang, Central Java, Indonesia in 1979. He received a bachelor's degree in physics education from Sebelas Maret University and a master's degree in science education from Semarang State University. Currently pursuing a doctoral degree in science education at Semarang State University. From 2003 until now he has been a lecturer in the Physics Education Department at Sebelas Maret University. He is the author of 5 books, 15 book

chapters and more than 20 articles. His interest is mainly in spreadsheet modelling and computational thinking.

Bayu Utomo was born in Temanggung, Indonesia. He received a Bachelor's degree in Engineering Physics (B.Eng.) from Universitas Gadjah Mada, Indonesia, and a Master of Science (M.Sc.) in Energy Conversion and Management from the University of Nottingham, UK. He is a research staff with the Indonesian Institute of Sciences. Since late 2020, he has been an Assistant Researcher with the Electrical, Energy, and Environment Research Group, National Research and Innovation Agency (BRIN), Indonesia. His research interests include phase change materials and their application in thermal management systems, cooling systems and power enhancement on photovoltaic, and reliability energy tests for household appliances. He is currently taking a doctoral degree in University of Nottingham, UK.

Dani Harmanto is currently an Associate Professor of Aeronautical Engineering at De Montfort University, Leicester, United Kingdom. He gained his MSc and PhD in Automotive Engineering design and manufacture from Coventry University, United Kingdom. He has number of position as a Chief editorial journal publications in the UK and Indonesia. He has written number of book chapters in Indonesian language. His expertise covers Computational Fluid Dynamics, vehicle design, design optimisation and others such as education.